AUTOMATED POSITIONING SYSTEM FOR BENCHTOP

CHARACTERIZATION OF MULTINUCLEAR RF COILS

An Undergraduate Research Scholars Thesis

by

JEANPAUL POSSO

Submitted to the LAUNCH: Undergraduate Research office at
Texas A&M University
in partial fulfillment of requirements for the designation as an

UNDERGRADUATE RESEARCH SCHOLAR

Approved by
Faculty Research Advisor: Dr. Mary P. McDougall

May 2023

Major: Biomedical Engineering

RESEARCH COMPLIANCE CERTIFICATION

Research activities involving the use of human subjects, vertebrate animals, and/or biohazards must be reviewed and approved by the appropriate Texas A&M University regulatory research committee (i.e., IRB, IACUC, IBC) before the activity can commence. This requirement applies to activities conducted at Texas A&M and to activities conducted at non-Texas A&M facilities or institutions. In both cases, students are responsible for working with the relevant Texas A&M research compliance program to ensure and document that all Texas A&M compliance obligations are met before the study begins.

I, Jeanpaul Posso, certify that all research compliance requirements related to this Undergraduate Research Scholars thesis have been addressed with my Faculty Research Advisor prior to the collection of any data used in this final thesis submission.

This project did not require approval from the Texas A&M University Research Compliance & Biosafety office.

TABLE OF CONTENTS

ABSTRACT

Automated Positioning System for Benchtop Characterization of Multinuclear RF Coils

Jeanpaul Posso
Department of Biomedical Engineering
Texas A&M University

Faculty Research Advisor: Dr. Mary P. McDougall
Department of Biomedical Engineering
Texas A&M University

Radio frequency (RF) coils are utilized in Magnetic Resonance Imaging (MRI) to acquire images of a subject. The design of RF coils is a significant factor in the quality of the image produced encouraging their construction to be personalized to the subject and fine-tuned to produce an acceptable image. Consequently, RF coils are designed in a variety of sizes and can exhibit different behaviors depending on their application. For all RF coils, it is important to ensure that the expected behavior is exhibited by the coils. Verification is performed by benchtop testing that involves S_{21} measurements with a network analyzer, where a signal is transmitted through the coil in question and a loop probe measures the magnitude of the transmit magnetic field (B_1^+). The effectiveness of the coil for the desired frequency with respect to the spatial location of the measurements is evaluated from the data acquired and can be visualized by generating a field map of the B_1^+ field.

Performing benchtop measurements has proven to be a time-consuming process that can produce inconsistent results when performed by hand as it is difficult to ensure that measurements are taken in equal spacing. To overcome this issue, companies have created

commercial models that can perform these measurements, but these models are costly. Other automated systems exist but they are limited to taking measurements for one frequency at a time or taking measurements for the B_0 field, or both. This thesis proposes an alternative system that allows for measurements to be performed in an automated or manual manner with precision and the capability of measuring multiple frequencies while being less expensive than existing solutions in the market. The effectiveness of this solution was evaluated by creating B_1^+ field maps for a birdcage coil and a loop coil using the various functions provided by the system and comparing the results to the expected behavior of the B_1^+ field for these coils. Results demonstrated that the system provides repeatable measurements, and it is capable of measuring coils of different geometries and with multiple frequencies while also providing a manual option for the user to utilize.

DEDICATION

To my parents, who have supported me throughout my academic career and have always wanted the best for me. To my sisters, to show that with enough effort and perseverance, they too can accomplish great things.

ACKNOWLEDGEMENTS

Contributors

I would like to thank my faculty advisor, Dr. Mary P. McDougall, for her guidance and support throughout the course of this research and for giving me the opportunity to work on this project.

I would also like to thank my colleagues who have been beneficial to my development as a researcher and have provided a learning environment.

The radio frequency birdcage coil tested in this study was provided by Joseph Busher. The radio frequency loop coil tested in this study was provided by Reagan Isbell and Vy Chu. The mechanical system was created by Carla Bassil. The MATLAB GUI, including the manual control option and the automated circle function, and the movement functions from the Arduino script were written by Jacob Degitz.

All other work conducted for the thesis was completed by the student independently.

Funding Sources

NOMENCLATURE

B_0 Magnetic Field of MRI Scanner

B_1 Magnetic Field of RF Coil

B_1^+ Transmit Magnetic Field of RF Coil

IDE   Integrated Development Environment

M_0 Net Magnetization Field

MRI   Magnetic Resonance Imaging

RF   Radio Frequency

1. INTRODUCTION

Magnetic Resonance Imaging (MRI) is an imaging modality that allows for noninvasive imaging of the body, or an object being scanned. This system utilizes the magnetic field of the scanner or the B_0 field, to align the spins of a specific nucleus of interest within the subject with or against the B_0 field. An excess of these spins aligns with the B_0 field resulting in a net magnetization field or the M_0 field, which is the source of signal imaged in MRI systems. To acquire a detectable signal, the M_0 must be "tipped" to align the plane transverse to the B_0 field. The radio frequency (RF) magnetic fields (B_1 fields) produced by coils are what perform this "tipping" function, and, in many cases, also act as the detector of the signal produced.

RF coils are designed to resonate at the Larmor frequency, a frequency that is dependent on the gyromagnetic ratio of the nucleus being imaged and the strength of the scanner's B_0 field. Transmitting RF energy at the proper resonant frequency tips the M_0 field into the transverse plane and signal is acquired. RF coils are designed in varying sizes depending on the subject of interest and application. To meet the needs of the imaging application, different types of coils can be made such as volume coils or surface coils. Research in this field has led to the exploration of coils to be tuned to more than one frequency. Multinuclear coils allow for multiple nuclei to be used as sources for imaging without having to change the coil and reposition the object being imaged [1].

To verify if RF coils are functioning properly, benchtop measurements are performed to map out the transmit magnetic field or the B_1^+ field. A loop probe is connected to a network analyzer and is positioned perpendicular to the expected B_1^+ field to measure the magnitude of the field at a specific location. A collection of measurements at different locations can be used to

produce a field map of the magnitude of the B_1^+ field. Previously, this was performed by hand, but these attempts proved to be time-consuming, and results were inconsistent. To overcome this issue, automated systems have been created, but commercial models are expensive [2-3]. Moreover, systems have been created for measuring the B_1^+ or B_0 field but they have been limited to measurements for one frequency at a time [3-5]. This project proposes an inexpensive alternative to existing automated models that ensures measurements of the B_1^+ field with consistency in data collection, precision in movement, and compatibility for coils of different sizes and shapes as well as multinuclear designs.

To test the effectiveness of this system, multiple RF coils will be measured including a birdcage coil and a loop coil. The birdcage coil is a volume coil that produces a homogenous magnetic field within the coil [6]. The birdcage also has other resonant modes that do not exhibit a homogenous magnetic field at other measurable frequencies, and field mapping is a method to determine at which frequency the homogeneous mode occurs [7]. The loop coil is a surface coil that produces a magnetic field that flows through the loop and wraps around the coil [8]. Considering these behaviors, the field maps generated using the proposed system will be evaluated to see if they resemble a reasonable field map for the tested RF coil. Successful representations of the B_1^+ magnetic fields suggests that the system is working correctly.

2. METHODS

The automated system consists of a mechanical, hardware, and software subsystems that operate together to provide quick and consistent measurements for RF coils. The design was chosen to account for coils of varying geometries and sizes as well as coils that are single-tuned or multi-tuned. The system was intended to be utilized by research laboratories with an interest in MRI hardware. Therefore, it is assumed that the laboratory has access to a network analyzer since it is an important tool in RF coil design as well as access to the necessary tools and materials to build loop probes.

Figure 1: Automated Measuring System

2.1   Mechanical System

The frame of the automated system was built with aluminum 80/20 extensions, and it has 4 wheels on the bottom for movement. The working surface was made of plywood (1.19 cm thick) and it offered a volume of 76.2 cm by 93.98 cm by 50.8 cm where the height can be adjusted as needed. Supports can also be added to shorten the gap between a coil and a probe. Three NEMA 17 stepper motors (Wantai Stepper Motors) are responsible for the movement of the loop probe where each motor drives a toothed belt. Set screws hold the gears onto the shaft of the motors and the gears are intertwined with the teeth of the toothed belts. Two motors controlled the movement in the X-axis and one motor controlled the movement in the Y-axis. Each motor of the X-axis moved a carrier on their toothed belt which held the Y-axis while the motor on the Y-axis moved the probe carrier. The three motors are powered by an external 12V power supply. An image of the automated system can be seen in **Figure 2**.
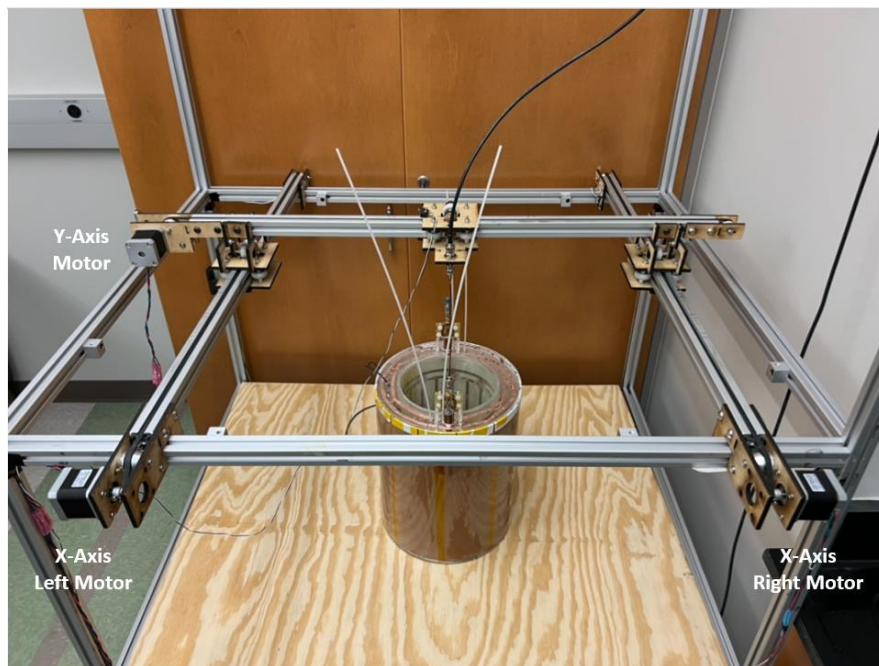
Figure 2: Mechanical System

2.2   Hardware System

The hardware subsystem consisted of a motherboard (RAMBo board), 3 motors, network analyzer, and a loop probe. The RAMBo board was connected to a personal computer using a USB Type B to USB Type A cable, the motors, and the network analyzer (Agilent E5071C). 4 pin connectors were added to the end of each motor prior to connecting each motor to their corresponding motor port on the RAMBO board. Connection between the RAMBo board and the network analyzer was established using custom length BNC cables and a custom circuit shown in **Figure 3**. The custom circuit regulated the output trigger signal from the RAMBo board using a voltage regulator and capacitor to avoid damage to the network analyzer. The regulated signal was sent through a custom length BNC cable to the external trigger input of the rear panel of the network analyzer. After measurements are completed, a trigger signal was sent from the external trigger output found at the rear panel and through another custom length BNC cable connected to the custom circuit. The circuit split the BNC so that signal and ground could connect to separate jumper wires plugged into the RAMBo board. The loop probe was attached to a female-to-female BNC adaptor that was tightened with a nut bulkhead on the probe carrier responsible for holding the probe. The other side of the connector was attached to the network analyzer using a BNC cable.
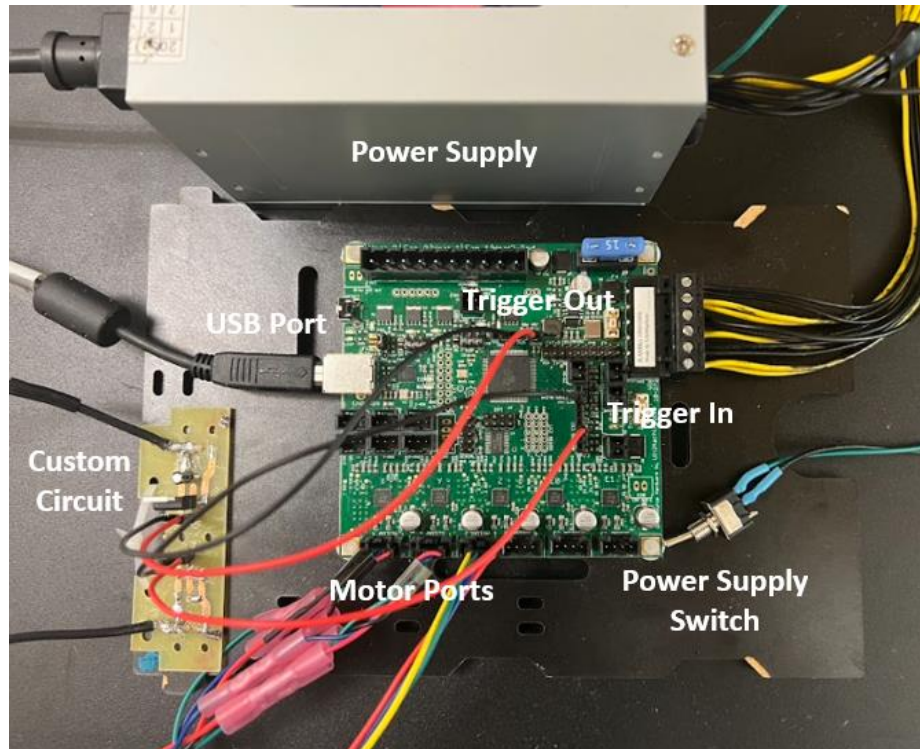
Figure 3: RAMBo Board and Custom Circuit

2.3   Software System

To operate the automated system, the coding languages Arduino, MATLAB, and VBA were utilized. An Arduino script and MATLAB GUI were run on a personal computer while the VBA script was run on the network analyzer. For proper use of this system, the Arduino script was uploaded and compiled to the RAMBo board prior to the system's first automated or manual run. Parameters are provided to the MATLAB GUI, but the automation functionality was not run until after the VBA script was run. Following this sequence ensured all communication between the different components of the automated system was performed in the appropriate order. **Figure 4** demonstrates how all components of the software system interact with each other to produce a successful run for measurement collection.
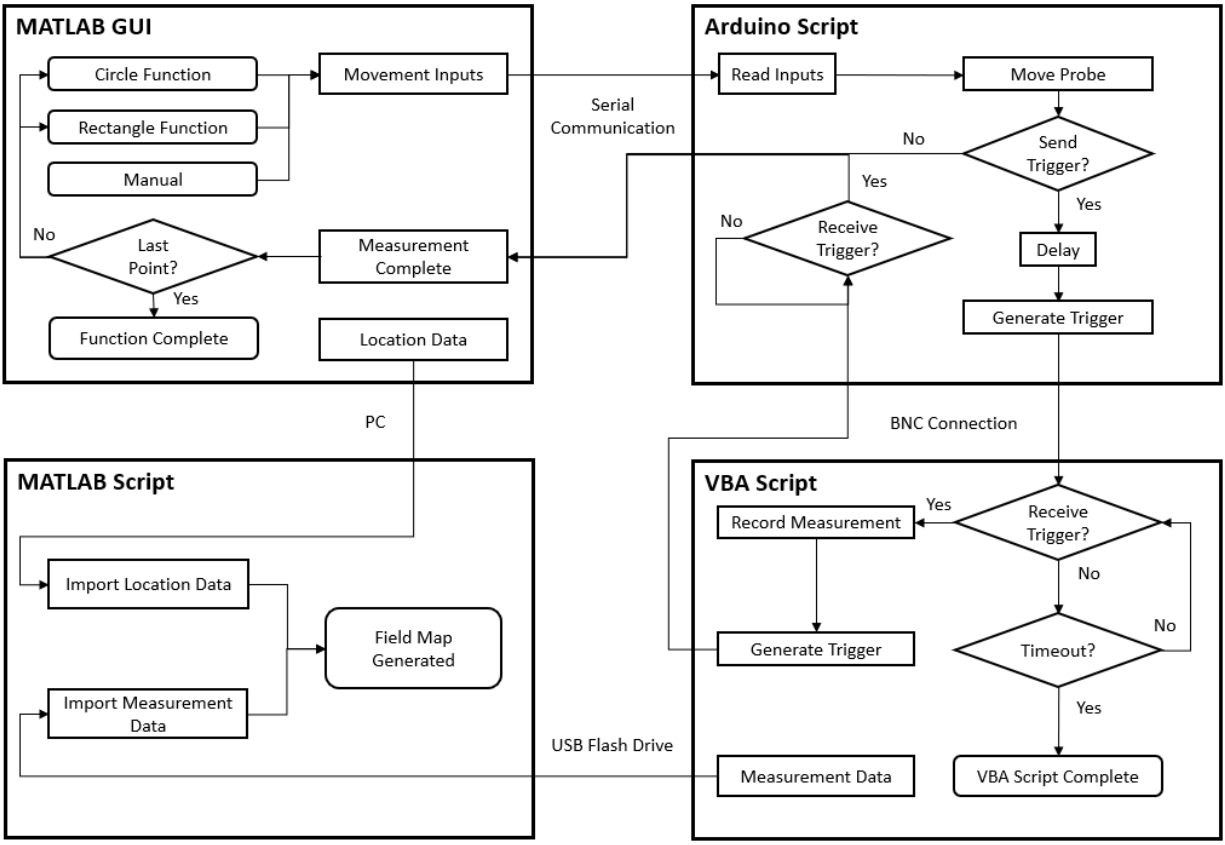
Figure 4: Software Flow Map

2.3.1   *Arduino Script*

The Arduino integrated development environment (IDE) was used to write the code for

the Arduino script, and a driver for the RAMBo Board was installed. Within this script, the ports

for the RAMBo Board were assigned and the functions for movement in the X-axis and Y-axis

given a distance and direction were defined. Apart from movement, the script was also

responsible for a function regarding communication between the RAMBO board and the network

analyzer through the use of trigger signals. This function generated a trigger signal from the

board to the network analyzer and waited until a signal was detected from the network analyzer

before continuing. Prior to sending a trigger, a 5 sec delay was implemented to allow for physical

stabilization of the loop probe. When a trigger was sent from the RAMBo board, this indicated

that a measurement must be taken at the current location of the loop probe. The trigger received from the network analyzer signified that the measurement was completed. Serial communication was established between the Arduino script and the MATLAB GUI for the purpose of passing information regarding the user's measurement request. The information received through the serial monitor was provided to the corresponding functions in the Arduino script.

2.3.2   MATLAB GUI and Script

The MATLAB IDE was used to create the GUI for the system and write the script responsible for generating the field map of the B_1^+ field. The MATLAB GUI provided the user with several measurement options based on the user's needs. For automated use, a circular function and rectangular function were available where for each function, the loop probe is commanded to follow a set path based on provided user inputs and the automated function that was selected. During this process, B_1^+ measurements were taken at points of interest. For the circular function, a resolution and radius were provided as user inputs and for the rectangular function, a resolution, length, and width were provided as user inputs. The manual option allowed the user to manually command the loop probe to move in a specified direction and distance for either the X or Y-axis.

The serial connection previously discussed between Arduino and MATLAB is turned on by first selecting the corresponding COM port and then changing the serial communication switch to its on state on the MATLAB GUI. Whenever the automated or manual options are selected, for each movement, a set of inputs are relayed from the MATLAB GUI to Arduino through serial communication. These inputs included the corresponding axis, direction, distance, and indications for a trigger to be sent for a measurement or if the current command is the final

command. For automatic movements, all inputs are used, while for manual movements, only the axis, direction and distance are utilized.

The MATLAB IDE was also used to write the script for generating field maps of the B_1^+ field. Prior to running the script, file locations for the file containing the location of the measurements and the file containing the measurement values must be written into the corresponding functions within the script. The resolution variable must also be updated to reflect the resolution used during the measurements. At the end of automated measurements, within the same folder as the MATLAB GUI, a CSV file is created containing the location of the loop probe whenever a trigger is sent. For manual measurements, values are manually written to a CSV file by the user performing the measurements.

2.3.3 VBA Script

VBA code was used to write a script used by the network analyzer. This script is responsible for a custom-made GUI and the procedures used by the network analyzer. On the GUI, the start button is clicked to set the network analyzer to its waiting for trigger state. If a trigger is received from the RAMBo board, the network analyzer acquires measurements for the frequency that the marker is set to. For multinuclear measurements, the corresponding variable for the number of markers in the script should be updated to reflect the number of markers needed. To ensure the correct data is collected, the user must ensure that the network analyzer is set up with the appropriate channel, trace, and frequencies for the markers. After the measurement is completed, the network analyzer sends a trigger back to the RAMBo board and it returns to its waiting for trigger state. After a set amount of time, if the network analyzer does not receive a trigger, it will display a message box indicating the end of the measurement process and a CSV file is completed and available containing the B_1^+ magnitude data. For multinuclear

14

coils, a CSV for each marker is produced, and the file is named based on the marker number. All measurement files can be transferred and retrieved from the network analyzer with a USB flash drive.

2.4   Measurement Set Up

2.4.1   Network Analyzer Calibration

For each coil, prior to acquiring measurements, the network analyzer ports that will be used were calibrated. Calibration was performed by connecting the BNC cables to an Electronic Calibration Module (Agilent Technologies) and selecting the ECal calibration function available with the network analyzer. When the ECal function was selected, it was set to calibrate for the two ports that would be used when connecting to the coil and the loop probe. Calibration could also be performed without the Electronic Calibration Module where the user instead would have to use another function on the network analyzer and attach a short, open, and 50 Ω load to the BNC cables that will be connected to the coil and the loop probe. Regardless of which calibration method is used, the sweep parameters on the network analyzer should be set for each coil prior to calibration to ensure accurate calibration for the range of frequencies of interest. Sweep parameters for the birdcage coil and loop coil can be seen in **Table 1**. Performing a calibration will overwrite the previous calibration on the network analyzer. Therefore, calibration and measurements were completed for one coil at a time.

Table 1: Network Analyzer Sweep Parameters for Birdcage and Loop Coils

RF Coil	Sweep Start	Sweep Center	Sweep End	Sweep Span	Number of Points
Birdcage	175 MHz	200 MHz	215 MHz	30 MHz	201
Loop	108 MHz	123 MHz	138 MHz	30 MHz	201

2.4.2   RF Coil Calibration

The birdcage coil and the loop coil were designed to resonate at 200 MHz and 123 MHz, respectively. To ensure that the birdcage and loop coils are set to these frequencies, the coils were tuned and matched, and an S_{11} measurement was taken. On the network analyzer, a marker was added for the resonant frequency and the format was changed to the Smith Chart (R + Jx). The variable capacitors of the coils were tuned with a tuning stick until the marker appeared at the center of the plot signifying a resistance of 50 Ω and reactance of 0 Ω. Changing the format to Log Mag provides an S_{11} measurement in dB where a value less than -20 dB is desired. The S_{11} measurement for the birdcage coil and the loop coil were -33.355 dB and -36.243 dB, respectively.

2.4.3   Network Analyzer Settings

On the network analyzer, the markers were set to the frequencies of interest and the parameters of the Trigger Menu were set. The parameters used for the Trigger Menu during the measurements can be seen in **Table 2.** The measurement type should be set to an S_{21} measurement where the BNC cable from port 1 is connected to the coil being tested and the BNC cable from port 2 is connected to the loop probe. The format of the measurement was set to Log Mag so that the markers would display their measurements in dB.

Table 2: Network Analyzer Trigger Menu Parameters

Parameter	State
Trigger Event	On Sweep
Trigger Scope	Active Channel
Ext Trig Input	ON
Low Latency	ON
Polarity	Positive Pulse
Position	After Point

2.5   Loop Probes

2.5.1 *Loop Probes for Experiments*

For the birdcage coil, a loop probe with a diameter of 2.4 cm and a length of 39.1 cm was made of a semi-rigid copper rod (EZ-86-CU/M17). A BNC connector was soldered at the end of the rod for direct connection to the probe carrier on the automated system. For the loop coil, a loop probe with a diameter of 0.7 cm and a length of 5.4 cm was made of a semi-rigid copper rod (EZ-47CU/M17) and the loop was bent to be perpendicular to the rod. A SMA connector was soldered at the end of the rod, requiring a male SMA to male BNC adaptor to connect to the probe carrier on the automated system. The probes used for the coils of interest can be seen in **Figure 5**.

Figure 5: Loop Probes for the Birdcage and Loop Coils

2.5.2 *Loop Probe Design*

To build the probes, one end of the semi-rigid copper rod was bent into a loop where there is enough length for the rod to wrap onto itself. Wrapping the rod around a cylindrical object can assist with this process. After the loop is acquired, at the end of the loop, a segment of the copper shielding is removed from the rod. This was accomplished by scoring the rod with a wire cutter followed by bending and pulling the scored section of the rod. Removing the copper shielding reveals a layer of dielectric and a signal pin at the center. Of the exposed length of dielectric, a portion of the dielectric was removed with a box cutter to expose the signal pin at the center. The signal pin was soldered onto to the same loop's copper shielding and two sections of the copper shielding were soldered to each other. The orientation of the loop is kept the same or bent based on the application for the probe. The straight edge of the probe was cut to the

18

desired length and the same approach to reveal the signal pin on the loop's end was applied to the straight edge. To connect the probe to the probe carrier of the automatic system, a BNC or SMA connector was soldered on to the straight edge of the probe, where an adaptor will be needed if a SMA connector is used. To solder the connector, a center pin is soldered to the signal pin of the semi-rigid and the center pin is inserted into the connector where it will clip into place. To ground the connector, the outer casing of the connector is soldered to the copper casing of the semi-rigid copper rod.

2.6 B_1^+ Measurement Acquisition

To demonstrate the capabilities of the automatic system, several measurements were run to test different aspects of the system. The RF coils involved in this study include a birdcage and a loop coil. The loop probe used varied based on the coil being evaluated. B_1^+ measurements acquired with the system were imported to the same MATLAB script to generate all field maps.

2.6.1   *Repeatable and Multi-Frequency Automated B_1^+Field Measurements*

To ensure that the proposed system can provide repeatable results, three sets of measurements were taken of the birdcage coil. To test the capability of measuring multiple frequencies, two markers were set during the measurements. The birdcage coil had an internal diameter of 17.8 cm and was tuned to 200 MHz. The first marker was tuned to 200 MHz and the second marker was set to 193.6 MHz which is the frequency of one of the birdcage's other resonant modes. The birdcage coil can be seen in **Figure 6**. Using the MATLAB GUI's manual option, the probe was positioned to be aligned with the center of the birdcage. On the MATLAB GUI, the parameters of the automatic circle function were set to a 10 mm resolution and a radius of 60 mm. The MATLAB GUI provided the location data of each measurement in a CSV file. The B_1^+ measurements were stored on the network analyzer as CSV files where the

19

measurements for 200 MHz and 193.6 MHz were recorded to separate CSV files. The field map

generation MATLAB script was used to create the B_1^+ field map for each set of data, where the

resolution in the script was set to 10 mm prior to running the script. To quantify the spread of the

measurements across the three trials for each frequency of interest, the standard deviation was

determined at each location and the average of these standard deviations was calculated. For the

measurements at 200 MHz, to evaluate the homogeneity of the B_1^+ measurements, the standard

deviation for each run was determined.
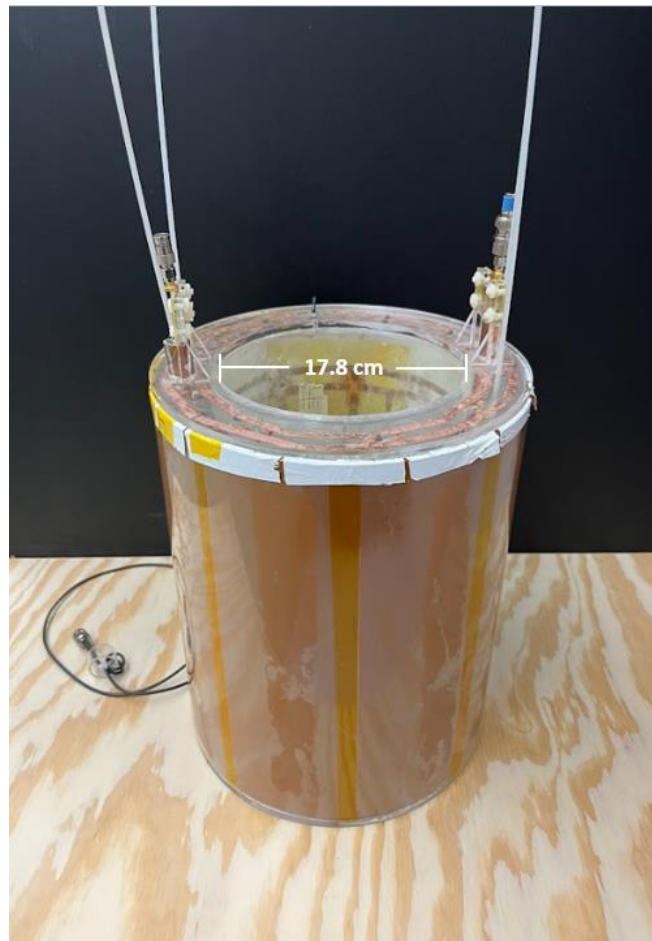
Figure 6: Birdcage Coil

*2.6.2   Automated and Manual B_1^+ Field Measurements of Birdcage Coil*

To evaluate whether the automatic and manual options of the system are comparable, B_1^+ field data was acquired for the birdcage coil using the manual option and then compared to the first set of data previously acquired with the automatic circle function for the same birdcage coil. To maintain similarity between the manual and automatic runs, the distance between the measurements and the locations within the loop at which the measurements were taken was the same between runs. During the manual run, at each point of interest, the network analyzer was internally triggered once, and the marker's value was recorded into a CSV file. The CSV file was formatted to follow the structure of the automatic run's CSV file. The loop probe that was previously used for the automatic run was also during the manual run. Using the field map generation MATLAB script, field maps were generated for each the manual and automatic run where the resolution in the script was set to 10 mm. Since both runs used the same location for measurements, the percent difference between the manual and automatic run at each point can be determined to determine whether there is a difference between the runs.

2.6.3   Automated B_1^+ Field Measurements of Loop Coil

To test the automated system's adaptability to different size coils and to test its automated rectangle function, measurements were taken of a loop coil. The coil had a diameter of 4 cm and was tuned to 123 MHz. The loop coil can be seen in **Figure 7**. Using the MATLAB GUI's manual option, the loop probe was positioned to be aligned with the center of the loop coil. To reduce the distance between the loop probe and the loop coil, the loop coil was placed on a support which shortened the gap between the probe and coil to 2.5 cm. On the MATLAB GUI, the parameters set for the automated rectangle function were a 5 mm resolution and an 80 mm length and width. The MATLAB GUI will produce a CSV file containing the location where the

measurements were taken, and the network analyzer will produce a CSV file with the B_1^+ field measurements. After the data was acquired, the field map generation MATLAB script was run to produce the field map. The resolution in this script was adjusted based on the resolution that was used during the measurement.
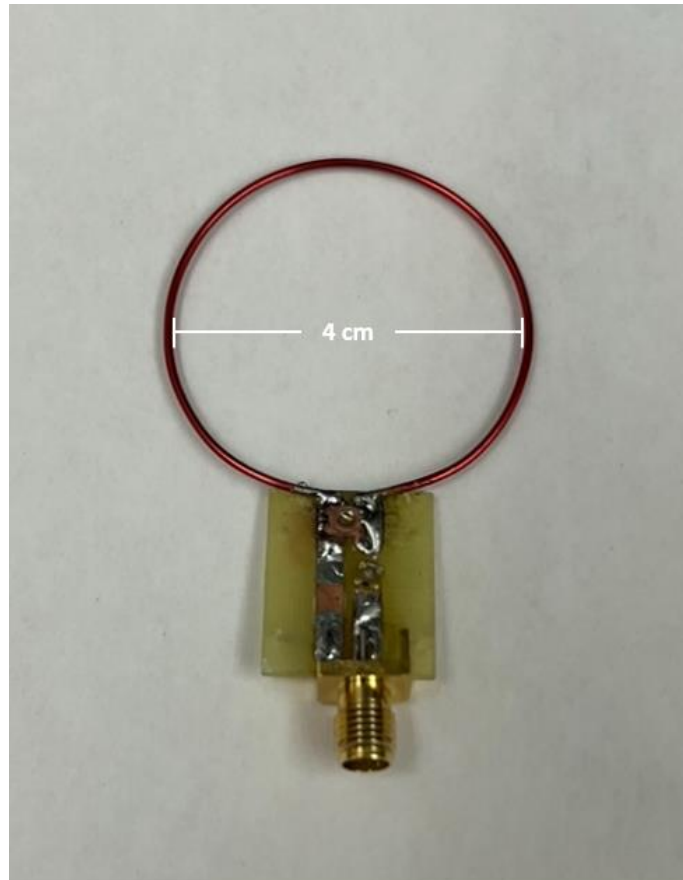
Figure 7: Loop Coil

2.7   System Resolution

To test the system's ability to produce high resolution measurements, the probe carrier was moved using the manual option of the MATLAB GUI at different resolutions, which were 1 mm, 5 mm, and 10 mm. For each resolution, the probe carrier was moved 10 times consecutively, and the distance between the starting position and the ending position was

measured. This process was repeated three times for each axis where measurements were taken for each individual motor. When the X-axis motors were tested, markings were done on the frame of the system next to the edge of the Y-axis carriers for the start and end positions. When the Y-axis motor was tested, markings were done next to the edge of the probe carrier for the start and end positions. The measured distances were compared to the expected distance to determine the percentage error for each resolution tested.

3. RESULTS

3.1 Repeated Automated B_1^+ Birdcage Date Acquisition

Three sets of B_1^+ measurements were obtained for the birdcage coil using the automatic circle function. B_1^+ field maps were generated for 200 MHz and 193.6 MHz and can be seen in **Figure 7** and **Figure 8**, respectively. The black squares in the figure represented locations where measurements were not taken while the X and Y-axis values represented the location of the probe. The intensity values represented the magnitude of the B_1^+ field measured by the network analyzer. Although a 5 second delay is present in the system for loop probe stabilization, this time was not sufficient for the loop probe to become completely still. For all measurements, error can be attributed to the loop probe's orientation and the slight inaccuracy of the motors.
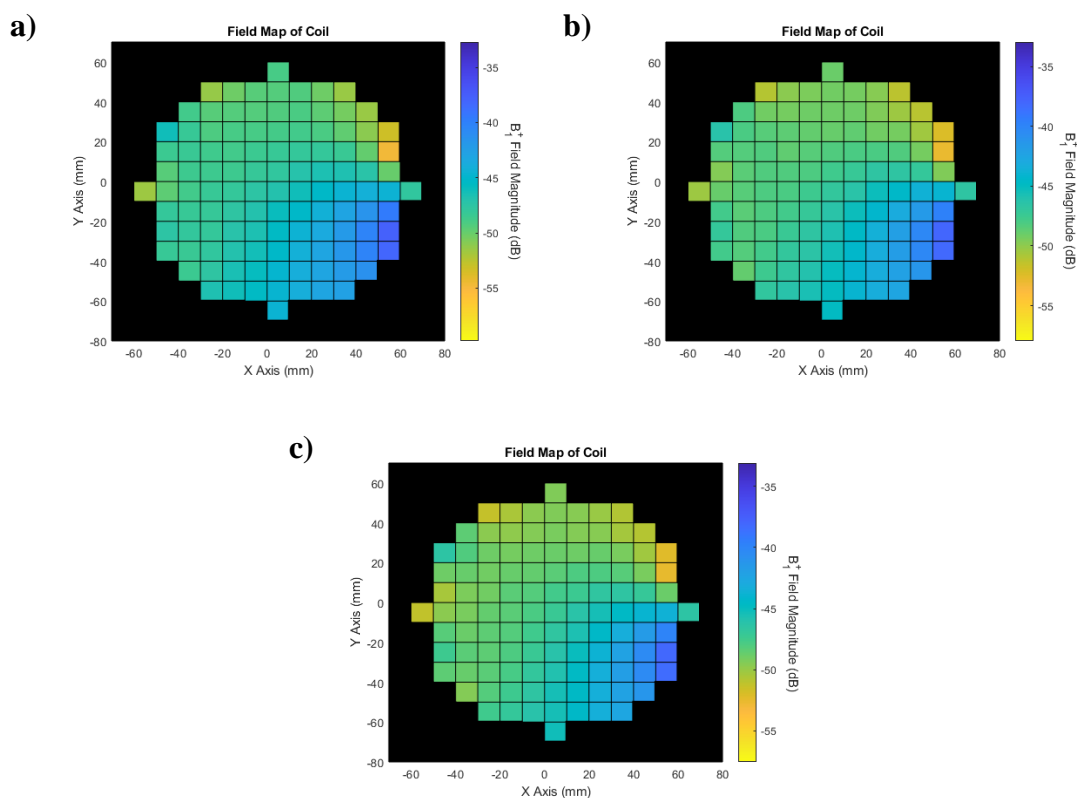

Figure 8: a) First, b) Second, and c) Third Automated B_1^+ Field Maps at 200MHz for Birdcage Coil
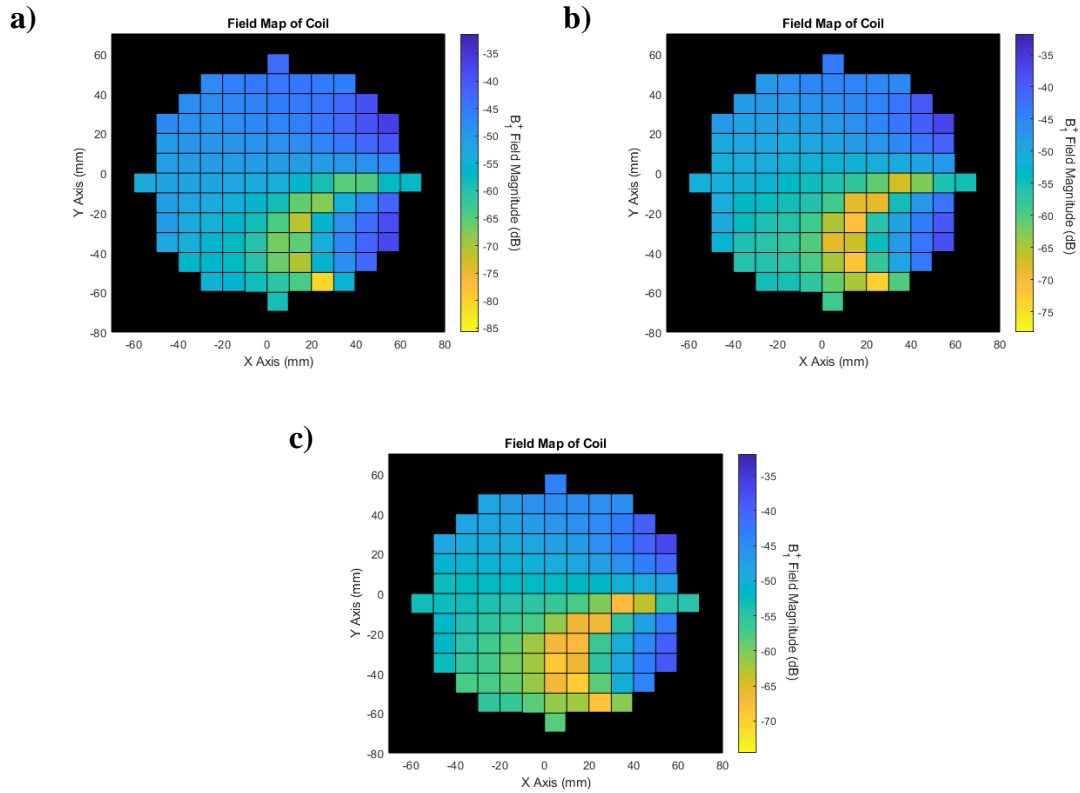
Figure 9: a) First, b) Second, and c) Third Automated B_1^+ Field Maps at 193.6 MHz for Birdcage Coil

For the field maps at 200 MHz, it was observed that the three runs exhibited a similar field distribution across the maps with an overall homogenous spread as expected for the birdcage [6]. For the field maps at 193.6 MHz, it was observed that the three runs exhibited a loss of signal in the bottom region of the maps. A loss of homogeneity is expected in the other resonant modes of the birdcage, suggesting these maps to be an appropriate representation of one of these modes [7].

The average standard deviations for the 200 MHz and 193.6 MHz data were 0.24 and 0.73. Since the standard deviations of the B_1^+ measurements were small, this suggests that the measurements acquired by the proposed system did not present a notable spread and it can be concluded that the measurements are repeatable. Repeatable results for both 200 MHz and 193.6 MHz also suggests that the system is capable of measuring the B_1^+ field of multiple frequencies

simultaneously. This is the same process that would be utilized for measuring multinuclear coils where each marker is set to a nucleus of interest. For the B_1^+ measurements at 200 MHz, the standard deviation of each run was determined and is shown in **Table 3**. Based on the low standard deviations, it can be determined that the spread of measurements is not large, and therefore the field is homogeneous.

Table 3: Standard Deviation of B_1^+ Field for Birdcage Coil at 200 MHz

Number of Run	Standard Deviation
1	3.02 dB
2	2.87 dB
3	2.88 dB

3.2 Automated and Manual Birdcage B_1^+ Data Acquisition

Manual and automatic B_1^+ measurements were acquired for the birdcage coil using the proposed system. The automated run of measurements was acquired using the automatic circle function while manual measurements were done using the manual option of the proposed system and manually triggering the network analyzer with single internal triggers. Field maps were generated from the data obtained and can be seen in **Figure 9**. In the figure, the black square represents points where measurements were not taken. The X and Y-axis values represent the location data provided by the MATLAB GUI after a run is performed. The intensity data represents the measurements taken by the network analyzer. One difference to note between the automatic and manual run is that the probe was able to stabilize completely before taking a measurement during the manual run unlike the measurements during the automatic run. Error in the measurements can be attributed to the orientation of the loop probe and the slight inaccuracy

26

of the motors. To quantify the difference between the runs, the percentage difference was taken

between the magnitude of B_1^+ fields at each point which resulted in an average percent difference
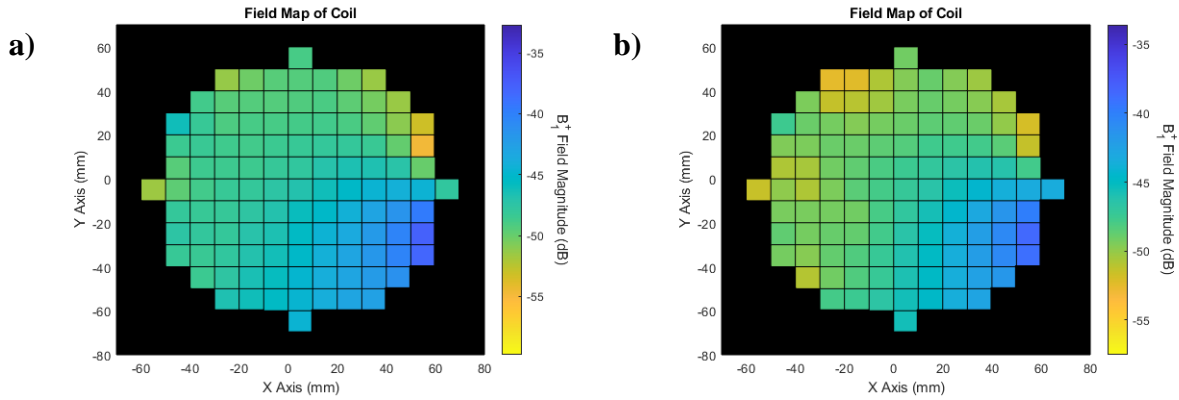
of 1.75%.

Figure 10: a) Automated and b) Manual B_1^+ Field Maps of Birdcage Coil

Upon inspection, the automatic and manual fields of the birdcage coil appear to have

similar color distribution throughout the map suggesting that the automatic and manual runs

produced similar results in terms of the homogeneity of the magnetic field. A homogenous

magnetic field is expected from a birdcage coil which is observed in the field maps of the

automatic and manual runs [6]. The average percent difference found between the B_1^+ magnitude

measurements suggests that the automated function was capable of recording similar results to

the manual run. Considering these results, both functions of the proposed system are able to

provide appropriate measurements for a given coil. When comparing these two options there are

some benefits for each. Manual control of the probe allows for the probe to move a distance and

direction set by the user so that specific areas or points of interest can be evaluated while

obtaining credible measurements. This comes at the inefficiency of having to manually record

measurement locations and B_1^+ magnitude data. Automatic control provides the options of

following a circular or rectangular path of variable sizes and resolutions while taking care of

writing down location and B_1^+ magnitude data. The disadvantage of this option is that the automatic functions are restricted to a circular or rectangular path which may not be applicable to all coils.

3.3   Automated Loop B_1^+ Data Acquisition

Automated B_1^+ measurements were taken from a loop coil using the automated rectangle function. The generated field map for the loop coil can be seen in **Figure 10**. The black squares represent points where measurements were not taken while the X-axis and Y-axis values represent the location of the probe during that measurement. The intensity values of the field map represent the measurements taken by network analyzer. Error can be attributed to the loop probe's orientation and the slight inaccuracy of the motors.
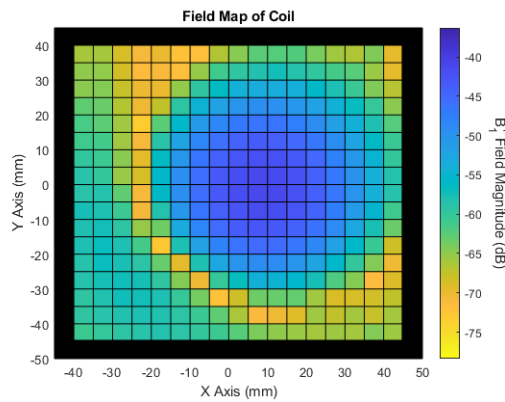

Figure 11: Automated B_1^+ Field Map of Loop Coil

When comparing the field map generated for the loop coil with the expected field map of a loop coil, there is a similarity in the behavior of the field within the loop where the field is at its strongest at the center and the magnitude drops as it gets closer to the edge of loop [9]. The length and width selected for the automatic rectangle function were chosen with the intention of having the probe take measurements within and beyond the loop. This can be seen in the bottom left corner of the map. A large drop in magnitude is expected when the loop probe is over the

28

loop since the direction of the B_1^+ field at these points should not be perpendicular to the loop

probe [8]. Measurements of the B_1^+ field should increase after the loop probe goes beyond the

loop since the direction of the field will be perpendicular to the loop probe [8]. Considering the

differences between the birdcage coil and the loop coil, the system used a finer resolution for the

loop coil which is a significantly smaller size than birdcage. Mapping the loop coil also provided

the opportunity to execute the automated rectangle function where the probe could measure the

B_1^+ field in the loop coil and beyond it, which was not possible with the birdcage due to its walls.

3.4   High Resolution Automated System

The percentage error for the system's movement by each motor for different resolutions

can be seen in **Table 4**. When comparing the percentage error across the three motors, it is

observed that the accuracy for each resolution remains consistent for the motors. When

comparing the percentage error between the resolutions, it is observed that for the resolutions of

5 mm and 10 mm, the percentage error remains less than 2%, suggesting that the system is

competent at taking B_1^+ measurements at these resolutions. For a 1 mm resolution, all the motors

presented a percentage error larger than the percentage errors of the other tested resolutions. Due

to this higher percentage error, it is not advisable to take measurements with a 1 mm resolution.

Motor	Resolution	Average Measured Distance	Expected Distance	Percentage Error
X-Axis (Left)	1 mm	9.02	10	9.80%
	5 mm	49.27	50	1.47%
	10 mm	98.63	100	1.37%
X-Axis (Right)	1 mm	9.18	10	8.23%
	5 mm	49.17	50	1.65%
	10 mm	98.61	100	1.39%
Y-Axis	1 mm	9.15	10	8.50%
	5 mm	49.34	50	1.33%
	10 mm	98.62	100	1.38%

3.5   Loop Probe Construction

When performing B_1^+ field measurements, the loop probes used varied depending on the geometry of the RF coils. For this study, the difference in size and shape between the birdcage and loop coil resulted in the need for different probes. Parameters that were considered during the construction of the loop probes include the loop diameter, rod length, rod thickness, and the orientation of the loop.

When choosing the size of the loop, it is important to consider the area that the probe must cover to capture the entire field of the coil. A loop probe that is small would result in a better resolution field map, but the overall time to acquire the measurements can increase significantly. A loop probe that is large would require less time to acquire the measurements, but

the resolution can be poor or there can be significant overlap in measurements. The length of the rod chosen for the loop probe reflects the size of the coil and any physical restrictions caused by the shape of the coil. For the birdcage, due to its tall wall, it was necessary for the probe to be long to maintain the probe's loop at a height within the region of interest of the birdcage while allowing the probe to move. The loop coil does not present the same physical restrictions as the birdcage, so a shorter probe was utilized. It was also observed that the length and thickness of the probes affected the stability of the probe. If a probe is longer or thinner, the time required for the probe to stabilize would increase. A shorter or thicker probe would provide better stability for the probe. The thickness of the wire also determines the cross-sectional area of the wire, which is inversely related to the resistance of the probe [10]. The orientation of the loop is dependent on the orientation of the transmitted magnetic field produced by the coil that will be measured. The birdcage generates a magnetic field that is parallel to its openings while within the loop coil, a magnetic field is generated that is perpendicular to the loop [6, 8]. To accommodate for the orientation of the magnetic field produced by the loop coil, the loop on the probe was bent to be perpendicular to the loop coil.

4.   CONCLUSION

MRI is a noninvasive imaging modality used for imaging the body or a subject of interest. To successfully acquire a signal, RF coils are built to tip excess spins that are aligned to the magnetic field of the MRI scanner by producing a magnetic field of its own. RF coils resonate at the Larmor frequency for the given field strength of the scanner, and they are designed in various geometries and sizes. These differences are dependent on the application resulting in different types of coils such as the birdcage coil or loop coil. Exploration with RF coils has led to investigations of multi-tuned RF coils due to their capability of acquiring signal for multiple frequencies without having to move the object of interest which can be beneficial for certain imaging applications [1].

Benchtop measurements of B_1^+ for the RF coils are taken to ensure the coils are designed and are functioning properly. These measurements are acquired using a loop probe connected to a network analyzer and the data can be visualized as a field map. Previously this was done by hand, but this has shown to be a time-consuming process that produces inconsistent data, and automated systems have been created, but commercial models are costly [2-3]. Existing models are able to measure the B_1^+ or the B_0 field, but only for one frequency at a time, prolonging the time required to fully characterize multinuclear coils since the process would have to be repeated for the other frequencies [3-5].

This study proposed a cheaper system that provides automated functionality with precise movement and compatibility for different geometry coils as well as multinuclear coils. Multiple automated measurements of the birdcage coil demonstrated the system's ability to provide repeatable results. The system was utilized to measure the B_1^+ field at different frequencies

showing its capability of characterizing multinuclear coils. To demonstrate its versatility for different coils, an automated circle and rectangle function were tested with different resolutions.

Future work for this system includes adding the functionality of a third axis and expanding on the characterization of probes. Adding a third axis allows the ability to gather measurements at different heights to obtain a more complete picture of the magnetic field. Considering the loop coil is a type of surface coil, an application for a third axis would be to map the B_1^+ field of the loop coil at different heights to determine or visualize its penetration depth [11]. As for characterizing the loop probes, multiple parameters that affect the performance of the probes have been discussed. A greater understanding of these parameters could lead to more optimal probe designs tailored to the coils being tested.

REFERENCES

[1]   A. Magill and R. Gruetter, Eds., "Nested Surface Coils for Multinuclear
        NMR," Encyclopedia of Magnetic Resonance, 2011, doi:
        https://doi.org/10.1002/9780470034590.emrstm1192.

[2]   "Magnetic Field Mapper, MMS-1-R," GMW Associates, 26-Oct-2021. [Online].
        Available: https://gmw.com/product/magnetic-field-mapper/#prettyPhoto. [Accessed: 23-
        Jan-2023].

[3]   M. Eisenmann, et al, "Development of a Low-Cost B0 Field Mapping Device," ISMRM
        2022, May 7 - 12 2022.

[4]   H. Han, R. Moritz, E. Oberacker, H. Waiczies, T. Niendorf, and L. Winter, "Open source
        3D multipurpose measurement system with submillimetre fidelity and first application in
        Magnetic Resonance," Nature News, 18-Oct-2017. [Online]. Available:
        https://www.nature.com/articles/s41598-017-13824-z. [Accessed: 23-Jan-2023].

[5]   Y. Ha, et al, "Automatic 3D B1 field mapping using 3D printer and digital oscilloscope
        for gradient-free MRI system," ISMRM & SMRT 2021, May 15 - 20 2021.

[6]   C. E. Hayes, W. A. Edelstein, J. F. Schenck, O. M. Mueller, and M. Eash, "An efficient,
        highly homogeneous radiofrequency coil for whole-body NMR imaging at 1.5
        T," Journal of Magnetic Resonance (1969), vol. 63, no. 3, pp. 622–628, Jul. 1985, doi:
        https://doi.org/10.1016/0022-2364(85)90257-4.

[7]   N. Gurler and Y. Ziya Ider, "FEM based Design and Simulation Tool for MRI Birdcage
        Coils including Eigenfrequency Analysis," COMSOL Conference Proceedings, 2012.

[8]   G. M. Baule and R. McFee, "The magnetic heart vector," American Heart Journal, vol.
        79, no. 2, pp. 223-236, 1970/2// 1970, doi: 10.1016/0002-8703(70)90312-1.

[9]   J. H. Kim, B. H. Choi, H. R. Kim, and C. T. Rim, "2-D Synthesized Magnetic Field
        Focusing Technology With Loop Coils Distributed in a Rectangular Formation," IEEE
        Transactions on Industrial Electronics, vol. 66, no. 7, pp. 5558–5566, Jul. 2019, doi:
        https://doi.org/10.1109/TIE.2018.2869362.

[10]   S. W. Ellingson, Electromagnetics, vol. 2, Blacksburg, VA, USA: Virginia Tech
         Publishing, 2020. [Online]. doi: https://doi.org/10.21061/electromagnetics-vol-1 CC BY-
         SA 4.0

[11]   A. M. Morey, S. Bhujade, T. Bhuiya, S. Thakur, and T. Pandey, "Design and
         development of surface coil for 1.5T MRI scanner," in 2015 International Conference on
         Smart Technologies and Management for Computing, Communication, Controls, Energy
         and Materials (ICSTM), 6-8 May 2015 2015, pp. 280-284, doi:
         10.1109/ICSTM.2015.7225428.